Geochemistry Geophysics Geosystems G3

Article
Volume 12, Number 3
29 March 2011
Q03011, doi:10.1029/2010GC003375
ISSN: 1525-2027

Published by AGU and the Geochemical Society

Solution and laser ablation inductively coupled plasma–mass spectrometry measurements of Br, I, Pb, Mn, Cd, Zn, and B in the organic skeleton of soft corals and black corals

B. Williams

School of Earth Sciences, Ohio State University, 125 South Oval Mall, Columbus, Ohio 43210, USA

Now at Department of Chemical and Physical Sciences, University of Toronto, South Building, Mississauga, Ontario L5L 1C6, Canada (branwen.williams@utoronto.ca)

A. G. Grottoli

School of Earth Sciences, Ohio State University, 125 South Oval Mall, Columbus, Ohio 43210, USA

[1] Proxy records can be derived from soft corals and black corals using minor and trace element measurements of the organic skeleton of these corals. Here, concentrations of Br, I, Pb, Mn, Cd, Zn, and B in the organic skeleton were determined using solution inductively coupled plasma–mass spectrometry (ICP-MS) in one black coral from 5 m depth and two soft corals from 85 and 105 m depth collected from a reef offshore of Palau in the western tropical Pacific. Solution ICP-MS results indicate that concentrations of some elements vary as expected with depth (Cd and Mn) while others are taxa specific (I) or colony specific (Br, Pb, Zn, and B). The intensities of the same elements normalized to ^{13}C were also measured at high resolution using laser ablation (LA) ICP-MS along radial transects covering the lifespan of the colonies. The results here indicate that high-resolution LA ICP-MS elemental records in black corals could be more fully developed for paleoceanographic reconstructions. In contrast, results of the laser transects from the two soft corals were not reproducible for any of the elements, and no discernible patterns were detected that could be developed into reliable proxy records using the current LA ICP-MS method.

Components: 7500 words, 7 figures, 2 tables.

Keywords: black coral; soft coral; ICP-MS; marine proxy development; tropical Pacific; trace elements.

Index Terms: 4916 Paleoceanography: Corals (4220); 1065 Geochemistry: Major and trace element geochemistry.

Received 21 September 2010; **Revised** 27 January 2011; **Accepted** 4 February 2011; **Published** 29 March 2011.

Williams, B., and A. G. Grottoli (2011), Solution and laser ablation inductively coupled plasma–mass spectrometry measurements of Br, I, Pb, Mn, Cd, Zn, and B in the organic skeleton of soft corals and black corals, *Geochem. Geophys. Geosyst.*, *12*, Q03011, doi:10.1029/2010GC003375.

1. Introduction

[2] Stable isotope records from soft corals and black corals have been successfully used as proxy records of nutrient sources and biophysical processes in surface waters [*Sherwood and Risk*, 2007; *Williams and Grottoli*, 2010a; *Williams et al.*, 2007]. Some types of these corals form a proteinaceous skeleton with growth bands useful for chronological control [*Grange and Goldberg*, 1994; *Sherwood et al.*, 2005a], similar to scleractinian corals. In addition, they are widely distributed in the tropical Pacific from near surface to thousands of meters deep [*Fabricius and Alderslade*, 2001;

Moore et al., 1956]. In scleractinian corals, trace element measurements of the calcium carbonate skeleton have been used to reconstruct seawater temperature (Sr/Ca [*Beck et al.*, 1992; *Smith et al.*, 1979]), upwelling (Ba/Ca [*Lea et al.*, 1989] and Cd/Ca [*Matthews et al.*, 2008; *Shen et al.*, 1987], terrestrial runoff at coastal sites (Ba/Ca [*Tudhope et al.*, 1997]), and soil erosion (Y/Ca [*Lewis et al.*, 2007]). To date, similar research has focused on Sr/Ca and Mg/Ca ratios in the calcite skeleton that is present in some soft coral genera such as *Plexaurella, Primnoa*, and *Eunicella* [*Bond et al.*, 2005; *Sherwood et al.*, 2005b; *Weinbauer and Velimirovm*, 1995]. Such elemental proxy records have not been developed for soft corals and black corals as a result of perceived difficulties in subsampling trace elements in an organic skeleton at high resolution. In addition, the method of trace element incorporation into the organic skeleton of soft corals and black corals is unknown. Previous studies of elemental abundances in the organic skeleton of soft corals and black corals have instead focused on understanding their morphology and possible application as biomaterials [*Goldberg*, 1976; *Nowak et al.*, 2005]. For example, a recent study used electron and proton microprobes to qualitatively explore the spatial distribution of Br, I, Zn, Mg, Ca, Sr, C, P, and S in the skeleton of three black coral specimens from different locations to assess skeletal morphological features, but not to reconstruct environmental conditions [*Nowak et al.*, 2009].

[3] To date, no high-resolution elemental analyses of the organic skeleton of soft corals or quantitative comparisons of trace elements concentrations between the organic skeletons of soft corals and black corals have been performed. If trace elements are incorporated into the skeleton in response to ambient seawater concentrations or environmental conditions, then these corals may provide an opportunity to reconstruct paleoceanographic conditions across a wide depth and geographic range. Therefore, the goals of this paper were to (1) quantitatively establish the concentrations of minor (Br, I) and trace elements (Pb, Mn, Cd, Zn, and B) in the organic skeleton of tropical Pacific soft corals and black corals collected along a 105 m depth transect and (2) evaluate the use of high-resolution LA ICP-MS measurements of Pb, Mn, Cd, Zn, and B for possible use as paleoceanographic proxy recorders. As a first-order approach, Pb and Cd were selected because concentrations of these elements increase with depth in the ocean, and Mn and Zn were selected because concentrations of these elements decrease with depth [*Abe*, 2004; *Bruland*, 1983; *Klinkhammer and Bender*, 1980]. B was selected because of its linear relationship with salinity [*Barth*, 1998; *Couch*, 1971; *Lee et al.*, 2010]. Br and I were selected because preliminary analyses revealed high concentrations of these elements in the soft coral and the black coral skeletons, and because reported differences in these concentrations appear to be linked to the coral age [*Goldberg*, 1976, 1978].

[4] To address the first goal, the selected elements were measured by solution ICP-MS to accurately determine concentrations of the elements in the skeleton of one *Antipathes* black coral from 5 m depth and two *Muricella* soft corals from 85 and 105 m depth collected from Short Drop Off Reef offshore of Palau in the western tropical Pacific (Figure 1). Depth-controlled and order-controlled (i.e., black coral (Antipatharia) versus soft coral (Alcyonacea)) variations in element concentrations were evaluated. To address the second goal, three adjacent radial transects from a basal cross section of each of the three coral colonies were each measured five times each using LA ICP-MS to test for reproducibility and potential proxy applications of each element.

2. Methods

2.1. Specimen Collection

[5] Two coral colonies, one *Antipathes* black coral from 5 m and one *Muricella* soft coral from 85 m were collected in 2006 by a diver using SCUBA. One additional *Muricella* soft coral from 105 m was collected in 2008 by manned submersible. Colonies were collected from Short Drop Off (SDO, 7°16.4′N, 134°31.4′E), a 300 m vertical reef wall located 2 km offshore of Palau (Figure 1). The site is well flushed by the northward surface current flow driven by the North Equatorial Countercurrent in the winter and a southward flow driven by the Palau eddy in the summer and is subject to minimal terrestrial influence [*Heron et al.*, 2006]. SDO is subject to the open ocean conditions surrounding Palau: warm surface waters (>28°C), low salinity (<34 psu), and relatively low nutrient levels within the mixed layer [*Picaut et al.*, 1996; *Yoshikawa et al.*, 2006]. At 5 m depth, the *Antipathes* colony was located within the warm mixed layer, while the two *Muricella* colonies were located within the 55 to 200 m depth range where the thermocline vertically fluctuates (55 to 200 m) [*Colin*, 2001;

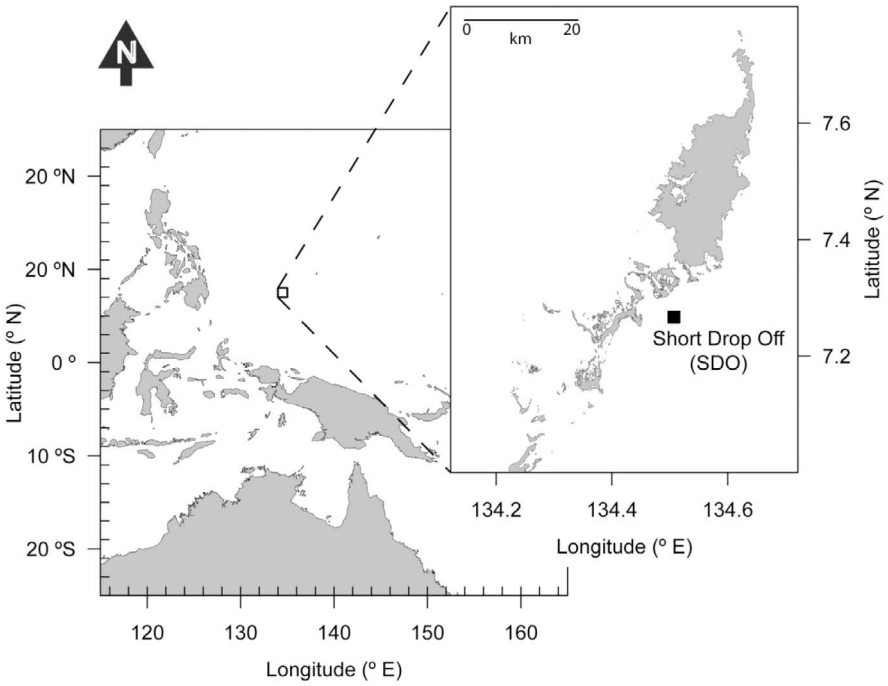

Figure 1. Map of western tropical Pacific, showing location of Palau and field site Short Drop Off. Courtesy of J. Watson.

Delcroix et al., 1996; *Iijima et al.*, 2005; *Zhang et al.*, 2007].

[6] All colonies were alive and in growth position when collected. An approximately 10 cm basal section was removed from each colony using large garden shears starting directly above the holdfast to just below the lowest branches. The *Antipathes* colony was identified by D. Opresko of the Oak Ridge National Laboratory. The *Muricella* colonies were identified according to *Fabricius and Alderslade* [2001] based on photos showing gross colony morphology, the morphology of sclerites under light microscope, and with the assistance of L. Colin at the Coral Reef Research Foundation, Palau.

2.2. Sample Preparation

[7] Two 1 cm thick cross-sectional slices were cut from the bases of the *Antipathes* colony and the *Muricella* colony from 85 m using a rock saw lubricated with water. The radial widths of these slices were 10.3 mm and 11.0 mm for the *Antipathes* and *Muricella* colonies, respectively. One cross section from each colony was sent to Calgary Rock and Mineral Services Inc. for thin sectioning to 30 μm and polishing. The remaining cross-sectional slices were prepared for elemental analysis. In addition, a 1 cm thick cross-sectional slice was cut from the *Muricella* colony from 105 m and prepared for elemental analysis. The radial width of this cross-sectional slice was 10.5 mm. To prepare the cross-sectional slices, the cut surface of each slice was smoothed using sandpaper attached to a Dremel drill. Loose skeletal material was removed with pressurized air. Each cross-sectional skeletal slice was rinsed three times using 18 mΩ Milli-Q water, cleaned in an ultrasonic bath for three 10 min periods, rinsed one additional time, and dried overnight at 40°C. A radial track for subsampling was selected for each specimen to optimize both the clearest banding patterns and the maximal radial distance across the cross-sectional slice.

2.3. Skeletal Imaging

[8] Thin sections from the *Antipathes* colony and the *Muricella* colony from 85 m were viewed under light microscope and photographed with an attached Nikon D80 Digital single-lens reflex camera with 10.2 Megapixel image size and 7.5 times optical zoom. The thin sections were also viewed and photographed using a Quanta200 Scanning Electron Microscope under high vacuum with a secondary electron detector in the Campus Electron Optics Facility at the Ohio State University (OSU). Photos of each thin section were

Table 1. Elements Analyzed by Solution ICP-MS[a]

Element (Isotope)	Mode	Known Value	Measured Value	±SE	RSD	Detection Limits	Method Blank
B (11)	Pulse	0.6	0.76	0.04	16	0.09	0.53
Mn (55)	Pulse	0.6	0.60	0.01	2.80	0.12	0.12
Zn (66, 68)	Pulse	12.0	11.90	0.15	3.91	0.30	1.92
Br (79, 81)	Analog	13333	9801	461	14	7046	1379
Cd (111, 112, 114)	Pulse	0.2	0.20	0.00	3.97	0.39	0.00
I (127)	Analog	100	568	272	144	9829	662
Pb (206, 207, 208)	Pulse	0.3	0.31	0.01	5.66	0.02	0.06

[a]Detection limits (DL) are calculated as 3 times the standard deviation of the instrument response to HNO_3. Method blanks of HNO_3 were subtracted from coral samples. Data are reported in ug g^{-1}.

spliced together using Adobe Photoshop CS2 software to create a single mosaic image for both of the colonies.

2.4. Solution ICP-MS

[9] To account for potential variation in trace element concentrations across growth rings within a basal cross-sectional slice of each colony, multiple skeletal samples were collected across a radial transect, analyzed by ICP-MS, and averaged to generate a representative concentration of each element for each colony. To do this, a radial transect across the basal cross-sectional slice of each colony was sampled at high resolution by milling at 0.1 mm increments using a high-precision, computer-driven Merchantek microdrill attached to an x, y, z controlled stage. The depth (~5 mm) and length (which varied along each transect from 0.5 cm to 1 cm) of the drilling path were set to minimize aliasing across time. Ten samples from the *Antipathes* colony, five samples from the *Muricella* colony from 85 m, and seven samples from the *Muricella* colony from 105 m were selected for solution ICP-MS analysis. Using a radiocarbon-derived chronology these samples were all selected from the period of 1966–2006 of each colony. A comprehensive description of the chronological development is given by *Williams and Grottoli* [2010a]. In brief, the chronology was developed by anchoring the start and the peak of bomb $\Delta^{14}C$ values in the coral skeleton to 1955 and 1979 in addition to the date of collection. The growth rate in mm yr^{-1} was calculated using these known points in time and assuming constant radial growth. Multiplying the radial width of the skeleton by the calculated growth rates resulted in ages of 38, 114, and 56 (±2) years for the *Antipathes* colony from 5 m and the *Muricella* colonies from 85 and 105 m, respectively.

[10] Approximately 0.5 mg of each skeletal sample was dissolved into 0.1 mL of double-distilled HNO_3 in an ultrasonic bath heated to 40°C for 6 h at which point the skeletal material was fully dissolved. Dissolved samples were spiked with ^{45}Sc, ^{103}Rh, and ^{81}Tl as internal standards, and the resulting solution was diluted to 1 mL with 18 mΩ Milli-Q water. A stock standard solution was made from single element standards and used to make five calibration standards spanning the expected range of element concentrations in the coral skeletons. All solutions were made in a Class 100 laminar flow hood. Two method blanks were collected by opening vials while at the microdrill station in the lab, capping them and then treated them the same as samples. These method blanks tested for laboratory contamination and the measured values were subtracted from the sample's values.

[11] All solution ICP-MS analyses were made on a Perkin-Elmer Sciex ELAN 6000 ICP-MS in the Trace Element Research Laboratory (TERL) at OSU. ^{79}Br, ^{81}Br, and ^{127}I were measured in analog mode. ^{206}Pb, ^{207}Pb, ^{208}Pb, ^{55}Mn, ^{111}Cd, ^{113}Cd, ^{114}Cd, ^{66}Zn, ^{68}Zn, and ^{11}B were measured in pulse mode. Calibration curves using the five stock solutions were created at the start, middle, and end of the analyses. HNO_3 blanks (n = 9) and external check standards (n = 9) were run every 3 to 5 samples. Precision of the check standards as indicated by the relative standard deviations (RSD) for each element varied by element and was <5% for Pb, Mn, Cd, and Zn, around 15% for Br and B, and was 140% for I (Table 1). Accuracy was <5% for Pb, Mn, Cd, and Zn as determined by comparing the measured check standard value with the nominal value of the stock solution. Accuracy was poor for Br and I (Table 1). Internal standards ^{45}Sc, ^{103}Rh, and ^{81}Tl accounted for instrumental drift over the duration of the analyses.

Table 2. LA ICP-MS Instrument Operating Parameters

Parameter	Setting
Laser	New Wave UP 193-HE laser system with homogenized beam
Pulse energy	~0.5 mJ
Repetition rate	10 Hz
Spot diameter at sample surface	50 μm
Laser fluence at sample surface	6.4 J cm^{-2}
Scan rate	10 μm s^{-1}
Center gas	0.8 L min^{-1} through ablation cell mixed with 1 L min Ar before injection into center of plasma
Plasma power	1150 Watts
ICP-MS	Thermofinnigan Element 2
Isotopes	^{11}B, ^{13}C, ^{55}Mn, ^{64}Zn, ^{79}Br, ^{114}Cd, ^{127}I, and ^{208}Pb
Mass spectral resolution	300

2.5. LA ICP-MS

[12] The isotopes ^{79}Br, ^{81}Br, ^{127}I, ^{208}Pb, ^{55}Mn, ^{114}Cd, ^{64}Zn, ^{11}B, and ^{13}C were measured across the radius of the cross-sectional basal skeletal slice of each coral colony by LA ICP-MS in the TERL at OSU. Each skeletal slice was mounted into an ablation cell with a motorized stage and scanned beneath a 193 nm ArF excimer laser with homogenizing beam (New Wave UP-193-HE) (Table 2). Three radial transects were selected from the center of the slice to the outer edge. At the sample surface, the laser beam had a 50 μm spot diameter. The laser was pulsed at 10 Hz and ~0.5 mJ cm^{-2}. Ablated material was carried to the plasma of a ThermoFinnigan Element 2 Inductively Coupled Plasma–Mass Spectrometer (ICP-MS) with fast magnet scan and high abundant sensitivity options via a continuous 0.8 L min^{-1} He stream that was mixed with 1.0 L min^{-1} Ar after the ablation cell. Plasma power was ~1150 W. Measurements were preceded and succeeded by ~20 s of background acquisitions. The ICP-MS was operated in medium mass spectral resolution (R = 300). Each section was scanned at a rate of ~10 μm/s. Autolock mass was used to minimize mass drift.

[13] Each radial transect was scanned six times. The first scan was considered a cleaning scan and the resulting data were discarded. Background measurements before and after each transect differed by <5% for B, C, Mn, Cd, and Pb, 10% for Zn, 17% for I, and 41% for Br. Higher background measurement of Br and I after scanning the samples resulted from slow washout times of these elements, and indicates limitations in using LA ICP-MS for high-resolution paleoceanographic reconstructions for these elements.

[14] Since suitable external standards have not been established for organic coral skeleton, isotopes in the synthetic glass standard reference material NIST 612 and the calcium carbonate standard MACS-1 were measured. The external standards were mounted in the ablation cell along with the *Antipathes* colony skeletal slice. Due to the size of the basal slices for the two *Muricella* colonies, the external standards were mounted into the ablation cell separate from the skeletal slice, and were analyzed before and after each radial transect.

2.6. Data Analysis

[15] Elemental concentrations determined by solution ICP-MS were automatically scaled by the instrument software to account for the natural abundance of the specific isotope measured. For elements in which multiple isotopes were measured (i.e., Br, Pb, Cd, and Zn), the concentrations were determined by averaging the weighted value of each isotope measured for that element. All averages are reported ±1 standard error (SE).

[16] LA ICP-MS data for each element were converted to an ASCII file using the instrument software and then imported into an Excel spreadsheet for data manipulation. The cross-sectional slices for the two *Muricella* colonies had visible skeletal cracks parallel to some growth bands. The location of cracks were noted during the ablation scans and data from these locations were subsequently removed from the LA ICP-MS data so that the resulting data set only included measurements of background before and after the sample, and of the sample itself. Data were smoothed using a four point moving average to reduce any short-term variation in the resulting data set due to peak hopping. An average of the background signal obtained before each standard and sample mea-

surement was subtracted from the signals for each standard and sample. For I and Br, only the background signal before the standard and samples measurement was used. The resulting smoothed and background-corrected data for each element were then normalized to ^{13}C and multiplied by 1000. ^{13}C was used in this study as an internal standard to account for variability in the amount of material ablated by the laser. ^{13}C was chosen because the carbon content of black corals was presumed to be constant throughout the skeleton, and because ^{13}C has been successfully used as an internal standard in other studies of materials composed of organic matter [*Rege et al.*, 2005].

[17] After discarding the "cleaning" scan for each transect, the subsequent five scans were averaged together to yield one record per radial transect. For each specimen, three radial transects were generated so that the intracolony variability could be assessed. Linear correlation analysis examined the relationship between these three radial transects in each colony for each element using SAS software Version 8.02 of the SAS System for Windows (copyright C 1999–2001 SAS Institute Inc.; SAS and all other SAS Institute Inc. products and service names are registered trademarks or trademarks of SAS Institute Ind., Cary, NC, USA). Since suitable standards were not present that matrix match the skeleton of soft corals and black corals, calibration of the LA ICP-MS data to determine the skeletal concentration was not feasible. Therefore only intensity profiles were calculated for each element. Distance along the intensity profiles for each element of each colony was converted to time based on the radial width of each cross-sectional slice and the growth rates calculated from the ^{14}C-derived chronology for that colony. Intensity profiles that were reproducible within a colony and that significantly varied over the lifespan of a colony were interpolated to produce evenly spaced annual values using the Timer program from the Arand Software package (courtesy of Philip Howell, Brown University, http://www.ncdc.noaa.gov/paleo/softlib/arand/arand.html). The spectral energy was evaluated on the interpolated data sets with the mean value subtracted using the Spectral program from the Arand Software package.

3. Results

3.1. Coral Imaging

[18] Growth banding was observable in the cross-sectional slices of all colonies by visual inspection and in photographs of the *Antipathes* colony (Figure 2a) and the *Muricella* colony from 85 m (Figure 2b). Banding in the *Antipathes* colony was best viewed using SEM while banding in the *Muricella* colony was best viewed under light microscope. Preparation of the thin sections caused visible cracks between the skeletal growth bands that were tens of microns wide in the *Antipathes* colony and millimeters wide in *Muricella* colony (Figures 2a and 2b).

[19] Clarity of skeleton bands varied greatly in both colonies. In the *Antipathes* colony, bands were clearly delineated at the center of the basal cross-sectional slice, could be easily counted, and were generally brighter than bands in the outer portion of the cross-sectional slice (Figure 2a). Bands in the middle portion of the cross section were generally darker and less clear and the delineation of bands in this region was subjective. Radial growth was approximately symmetrical in this colony, with the largest source of variation resulting from skeletal cracks. In the *Muricella* colony, clear banding patterns were visible in some areas of the basal slice with band widths ranging from tens of microns to greater than one mm (Figure 2b). In some regions of the skeleton delineation between bands was subjective and a single band could not be clearly followed around the circumference of the slice. Radial growth was asymmetrical in this colony resulting in an oblong shape.

3.2. Solution ICP-MS Measurements

[20] Overall, Br and I concentrations were highest while the minor elements Pb and Mn were lowest (Figures 3a–3d) in all of the colonies. The skeletal I concentration was an order of magnitude higher in the *Antipathes* colony than in the two *Muricella* colonies (Figure 3b). Skeletal Br, Pb, and Cd concentrations increased with depth (Figures 3a, 3c, and 3e) and Zn concentrations were an order of magnitude higher in the deepest colony (Figure 3f). Br, Pb, Cd, and Zn increased by one and a half, nine, thirty, and seventeen times, respectively, between 5 and 105 m. Finally, [B] in the *Muricella* colony from 85 m was less than half as abundant as in the other two colonies (Figure 3g).

3.3. Laser Ablation ICP-MS Measurements

[21] The intensities of the five replicate scans within each radial transect were highly reproducible in all three transects within each colony (Figure 4). Therefore for each colony, the 5 replicate scans of each of the three transects were

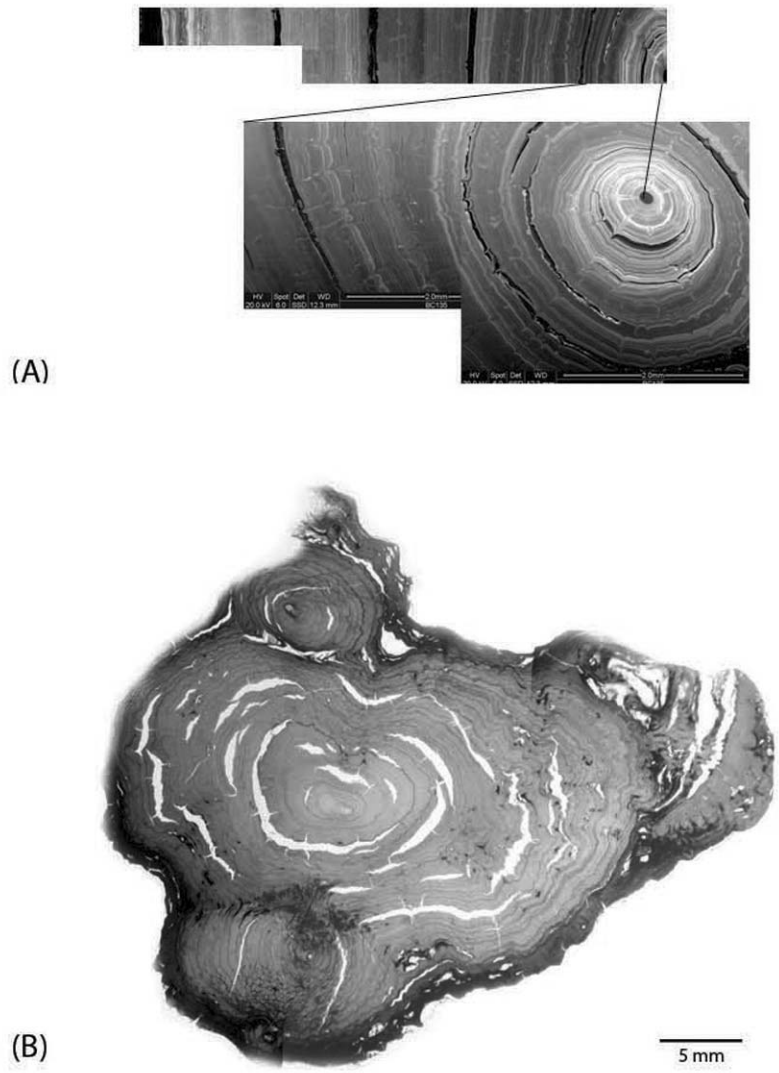

Figure 2. Photographs showing concentric growth bands in (a) the *Antipathes* colony from 5 m viewed under a scanning electron microscope and (b) the *Muricella* colony from 85 m viewed under a light microscope.

averaged to produce three approximately parallel radial transect profiles per colony.

[22] Within the *Antipathes* colony, the three radial transects were significantly correlated with each other for all elements (Pearson correlation coefficients of $r = 0.46$ to $r = 0.98$, $p < 0.0001$), confirming that they were very reproducible within the coral (Figure 5). This reproducibility among the three radial transects suggests that ^{13}C is constant in the skeleton and supports the application of ^{13}C as an internal standard. Overall, the following patterns were observed: (1) $^{79}Br/^{13}C$ intensities increased from the 1990s to the mid-2000s (Figure 5a); (2) $^{127}I/^{13}C$, $^{208}Pb/^{13}C$, and $^{114}Cd/^{13}C$ intensities were greatly elevated in the 1960s portion of the record (Figures 5b, 5c, and 5e); (3) a large peak in intensity of short duration in ~1983 was observed in a single transect for each of $^{55}Mn/^{13}C$, $^{114}Cd/^{13}C$, and $^{64}Zn/^{13}C$ (Figures 5d–5f); and (4) $^{11}B/^{13}C$ intensities varied on decadal scales over the lifespan of the coral (Figure 5g). Therefore, only the $^{11}B/^{13}C$ intensities were evaluated for spectral energy, which revealed no significant spectrum.

[23] The intensities of three radial transects in the *Muricella* colonies were not always reproducible (Figures 6 and 7) and the transects for many elements within each colony were not statistically

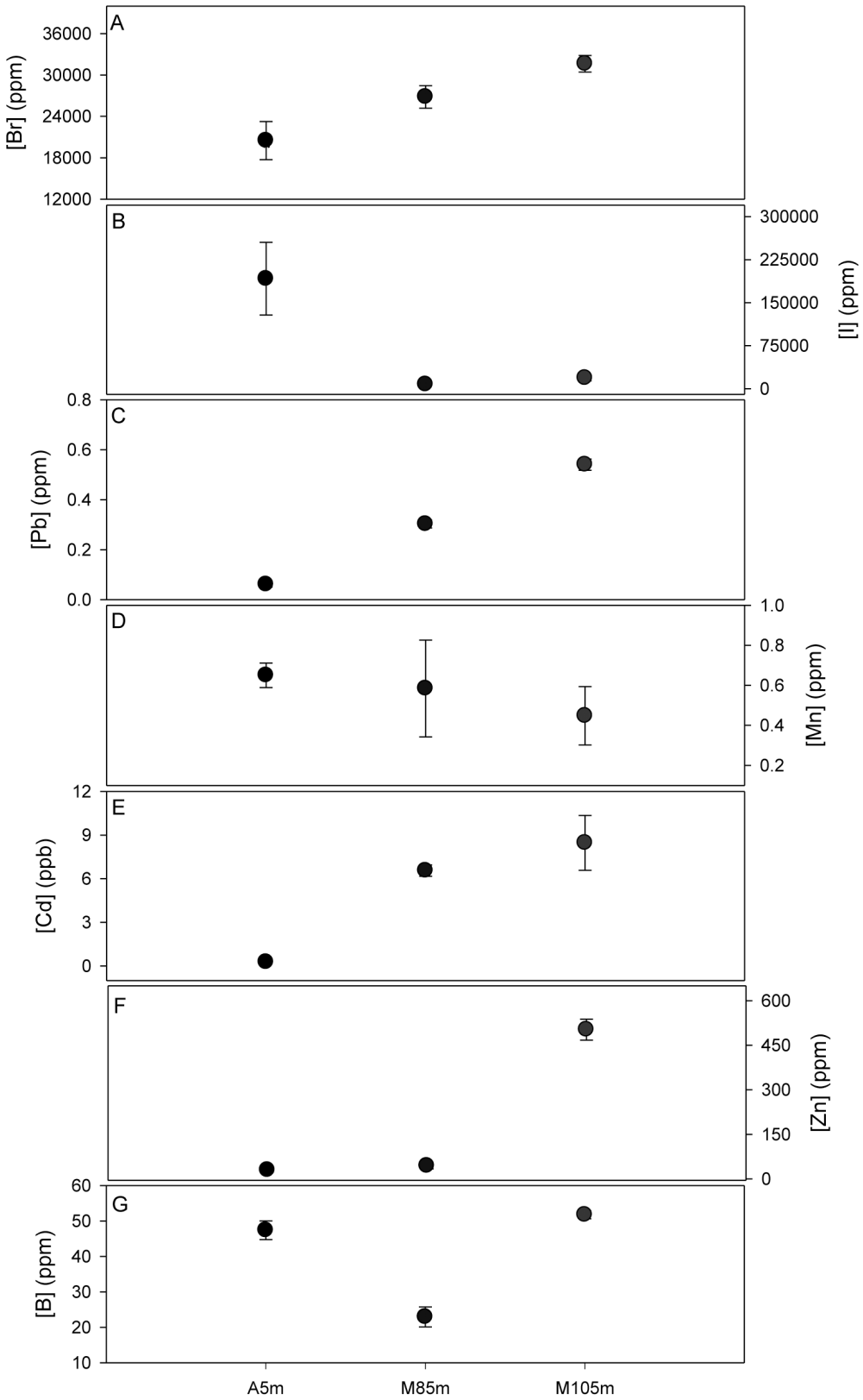

Figure 3. Average concentrations of the elements (a) Br, (b) I, (c) Pb, (d) Mn, (e) Cd, (f) Zn, and (g) B for the *Antipathes* colony from 5 m (n = 10), the *Muricella* colony from 85 m (n = 5), and the *Muricella* colony from 105 m (n = 7) for the common period 1966–2006. All averages are ±1 standard error.

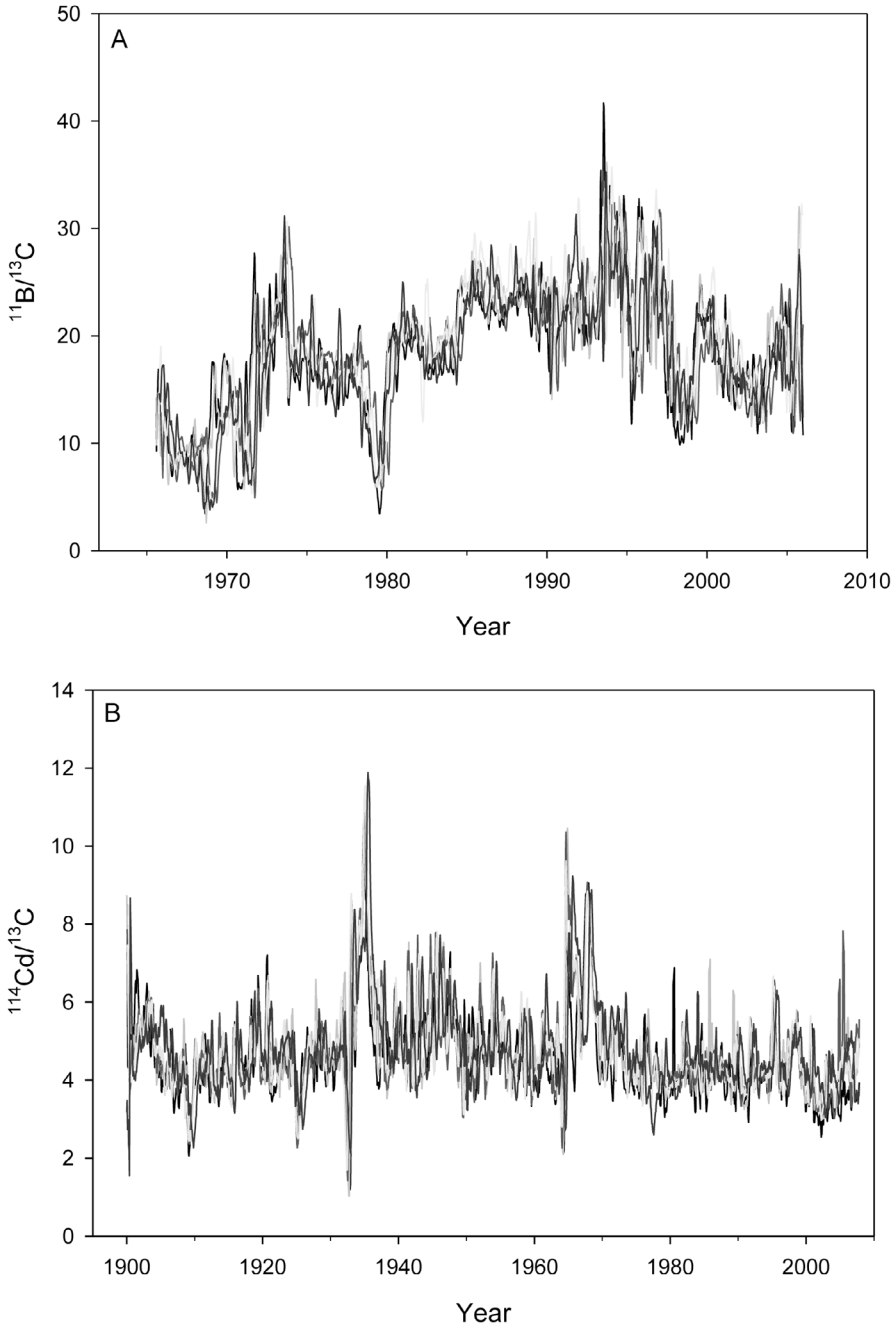

Figure 4. Examples of the high reproducibility of the five replicate scans for one radial transect. (a) Values of $^{11}B/^{13}C$ in the *Antipathes* colony from 5 m. (b) Values of $^{114}Cd/^{13}C$ in the *Muricella* colony from 85 m. All radial scans were smoothed with a four-point running mean, blank corrected, normalized to ^{13}C, and multiplied by 1000.

correlated. In the *Muricella* colony from 85 m, large negative anomalies in $^{79}Br/^{13}C$, $^{208}Pb/^{13}C$, $^{114}Cd/^{13}C$, and $^{11}B/^{13}C$ intensities were observed in one of the three transects in the 1970s (Figures 6a, 6c, 6e, and 6g). In two of the three transects, large positive departures of short duration in $^{127}I/^{13}C$ and $^{55}Mn/^{13}C$ intensities were present in the early 1990s (Figures 6b and 6d). In general, a gradual increase in $^{208}Pb/^{13}C$ was observed from the 1940s to the present (Figure 6c) while $^{55}Mn/^{13}C$, $^{64}Zn/^{13}C$, and $^{11}B/^{13}C$ intensities all increased in the youngest portion of the record post-1985 (Figures 6d, 6f, and 6g). In the *Muricella* colony from 105 m, $^{127}I/^{13}C$ and $^{55}Mn/^{13}C$ intensities were

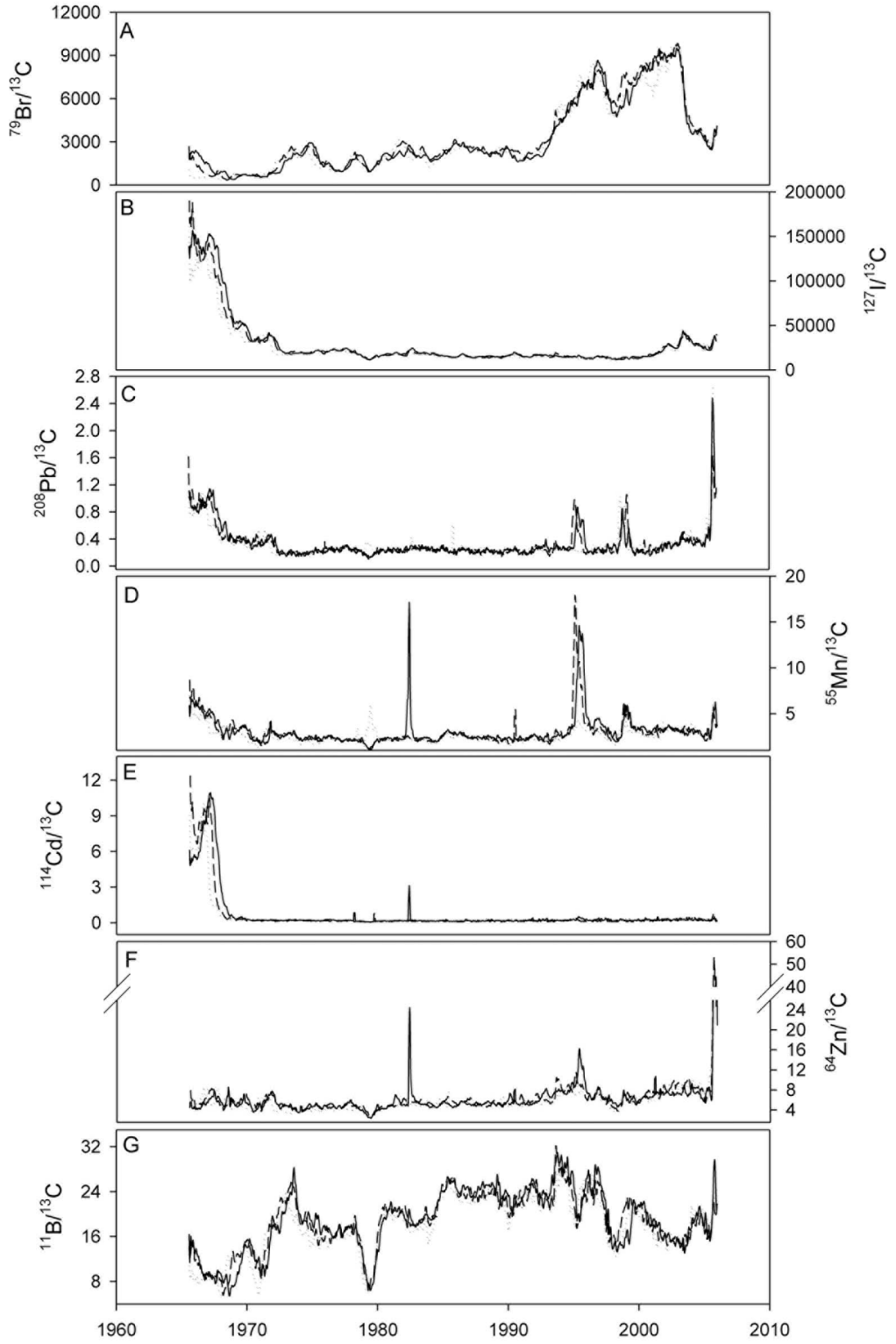

Figure 5. Three radial transects in the *Antipathes* colony from 5 m for the isotopes (a) $^{79}Br/^{13}C$, (b) $^{127}I/^{13}C$, (c) $^{208}Pb/^{13}C$, (d) $^{55}Mn/^{13}C$, (e) $^{114}Cd/^{13}C$, (f) $^{64}Zn/^{13}C$, and (g) $^{11}B/^{13}C$. Each isotope was smoothed with a four-point running mean, blank corrected, normalized to ^{13}C, and multiplied by 1000. Each radial transect is the average of five replicate scans.

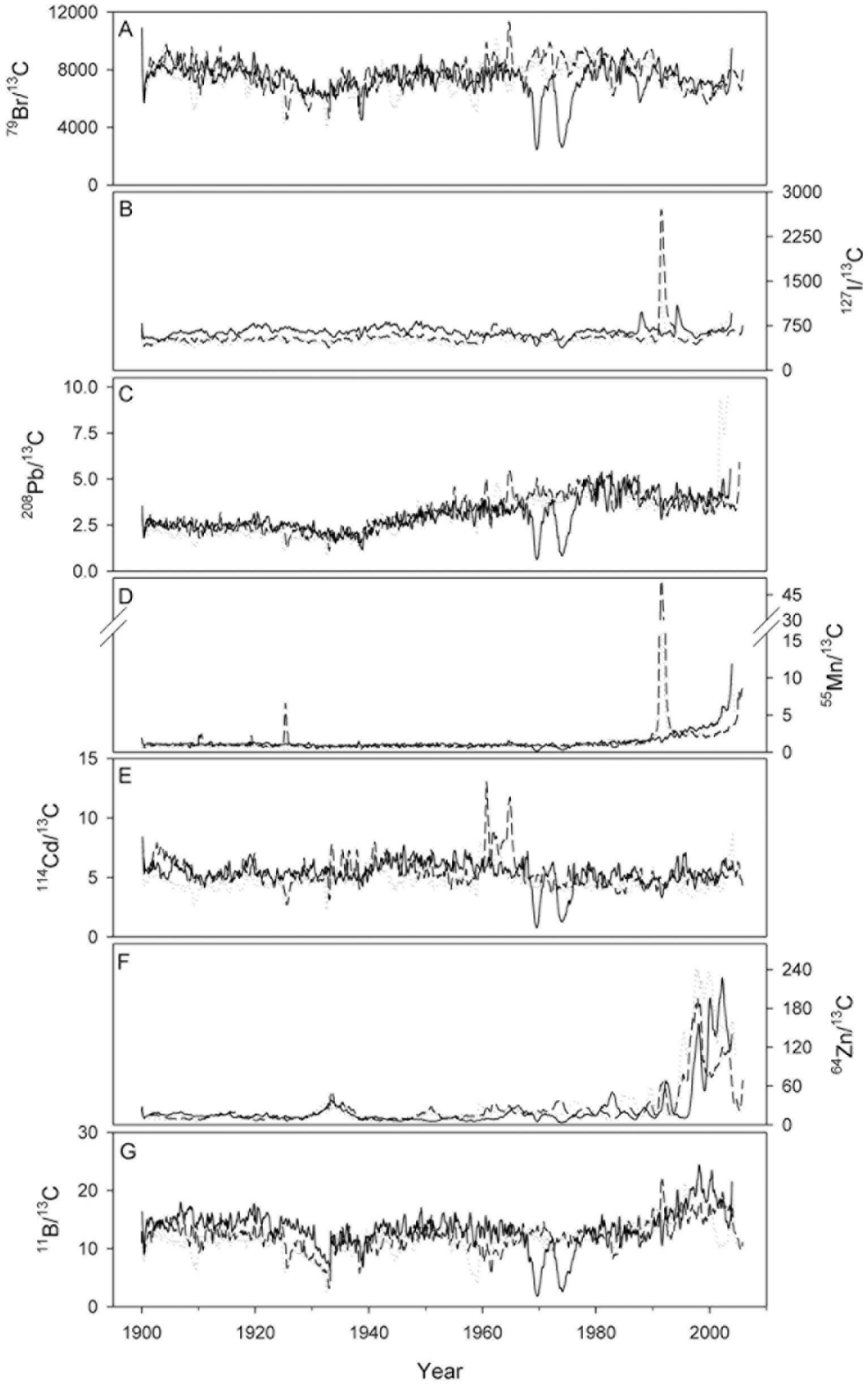

Figure 6. Three radial transects in the *Muricella* colony from 85 m for the isotopes (a) $^{79}Br/^{13}C$, (b) $^{127}I/^{13}C$, (c) $^{208}Pb/^{13}C$, (d) $^{55}Mn/^{13}C$, (e) $^{114}Cd/^{13}C$, (f) $^{64}Zn/^{13}C$, and (g) $^{11}B/^{13}C$. Each isotope was smoothed with a four-point running mean, blank corrected, normalized to ^{13}C, and multiplied by 1000. Each radial transect is the average of five replicate scans.

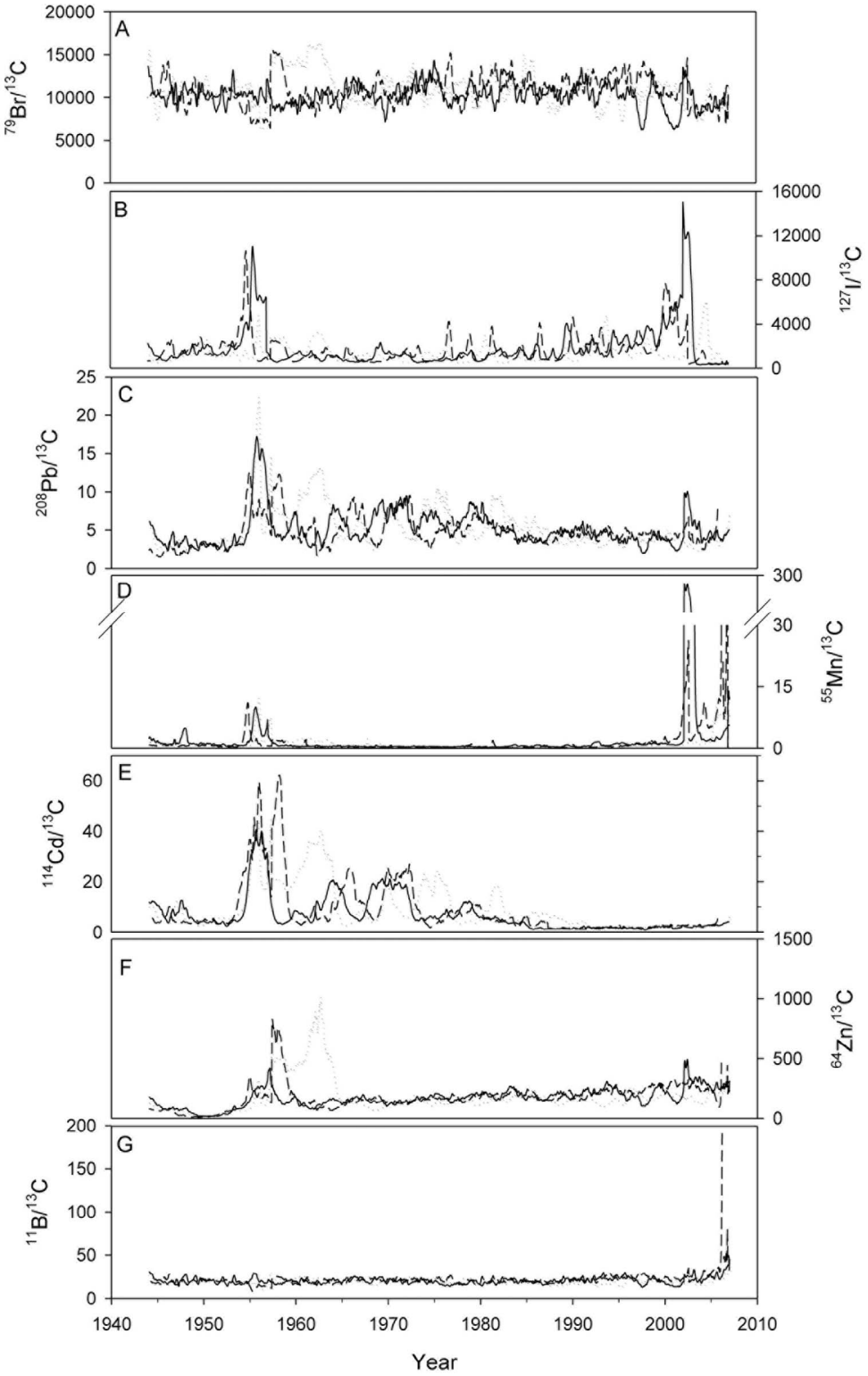

Figure 7. Three radial transects in the *Muricella* colony from 105 m for the isotopes (a) $^{79}Br/^{13}C$, (b) $^{127}I/^{13}C$, (c) $^{208}Pb/^{13}C$, (d) $^{55}Mn/^{13}C$, (e) $^{114}Cd/^{13}C$, (f) $^{64}Zn/^{13}C$, and (g) $^{11}B/^{13}C$. Each isotope was smoothed with a four-point running mean, blank corrected, normalized to ^{13}C, and multiplied by 1000. Each radial transect is the average of five replicate scans.

anomalously high in the mid-1950s and from 2000 to the end of the record (Figures 7b and 7d). In addition, $^{208}Pb/^{13}C$, $^{114}Cd/^{13}C$, and $^{64}Zn/^{13}C$ intensities were also anomalously high in the mid-1950s (Figures 7c, 7e, and 7f). Large fluctuations in $^{208}Pb/^{13}C$ and $^{114}Cd/^{13}C$ intensities started in the mid-1950s and slowly decreased in intensity until the 1990s (Figures 7c and 7e) while $^{11}B/^{13}C$ intensities doubled in magnitude in the last five years of the record (Figure 7g).

4. Discussion

[24] The source of trace elements and their method of incorporation into the skeletons of soft corals and black corals are unknown. However, the major elements carbon and nitrogen in the *Antipathes* and *Muricella* corals in this study were obtained heterotrophically from ambient suspended particulate organic matter (POM) in colonies within the euphotic zone from the western tropical Pacific [*Williams and Grottoli*, 2010b], and this is likely the primarily source of trace elements to these corals as well. However, trace element measurements of suspended POM through the euphotic zone in the western tropical Pacific are rare. POM elemental composition largely depends on the elemental concentrations in the plankton and/or elemental adsorption onto POM, both of which occur partly as a function of the concentrations of each element in seawater [*Boyle et al.*, 1976; *Fisher et al.*, 1987; *Härdstedt-Roméo*, 1982]. Therefore, if the concentrations of trace elements in POM reflect those of seawater, and if the corals incorporate trace elements directly from POM, then the concentrations of trace elements in the organic skeleton should reflect those of seawater. As a first-order approach, the trace element concentrations in the coral skeletons collected at various depths were compared to known changes in the concentrations of these trace elements in seawater with depth.

[25] Differences in the average elemental concentrations in the *Antipathes* coral and the *Muricella* corals could reflect either order-specific variability in skeletal geochemistry, colony-specific variability in skeletal geochemistry, offsets in concentration related to changes in seawater concentrations with depth, or some combination of two or more of these possibilities. In addition, changes in element concentrations within a single colony over time (i.e., across a radial transect) could reflect either variability in the biology of the coral colony itself, variability in response to ambient environmental conditions, or both. All of these possible sources of elemental variability in the soft and black coral skeletons are further explored below.

4.1. Solution ICP-MS Element Concentrations

[26] The high halogen contents (Br and I) measured here (Figures 3a and 3b) are consistent with the results of previous studies on soft corals and black corals using analytical methods other than ICP-MS [*Cook*, 1904; *Goldberg*, 1978; *Goldberg et al.*, 1994; *Nowak et al.*, 2009; *Roche*, 1952; *Sugimoto*, 1928]. However, *Goldberg* [1978] reported similar concentrations of I and Br in soft corals while our data show that [Br] are higher than [I] in the *Muricella* colonies (Figures 3a and 3b). In addition, the [Br] increases with depth in these colonies although seawater [Br] does not change with depth [*Morris and Riley*, 1966]. Therefore, although high [Br] and [I] values are characteristic of these corals, concentrations of I appear to be influenced by order-specific effects (Figure 3b) and Br appears to be influenced by colony-specific effects (Figure 3a). Consequently, Br and I have limited use for paleoceanographic reconstructions.

[27] Order-specific variability does not drive skeletal [Pb] since it varies significantly between all three colonies (Figure 3c). Low [Pb] in the *Antipathes* colony from 5 m and high [Pb] in the deepest *Muricella* colony from 105 m (Figure 3c) is not consistent with higher [Pb] in surface water supplied by atmospheric input but could reflect a subsurface maxima in [Pb] at several hundreds of meters deep in the central Pacific [*Flegal and Patterson*, 1983]. The large increase in [Pb] between the 85 and 105 m specimens, however, suggests that specimen-specific variability drives the increase in [Pb] with depth. Lower skeletal [Cd] in the *Antipathes* colony compared to the two deeper *Muricella* corals (Figure 3e) could be an order-specific effect or a depth effect. Ambient [Cd] in seawater is depleted at the surface due to biological activity [*Xu et al.*, 2008], while the remineralization of sinking organic material increases [Cd] at depth [*Boyle et al.*, 1976], so a depth effect is likely. Similarly, high skeletal [Mn] in the *Antipathes* colony and low [Mn] in the deepest *Muricella* colony is consistent with higher [Mn] in surface waters, supplied by atmospheric dust deposition (Figure 3d) [*Klinkhammer and Bender*, 1980]. Therefore, while order-specific effects cannot be ruled out for [Cd], increasing [Cd] and decreasing [Mn] with depth appear to reflect ambient concentrations in seawater. If ambient concentrations do drive skeletal concentrations of

these elements, then as a first-order suggestion, these elements may be useful for paleoceanographic reconstructions.

[28] Order-specific variability does not drive skeletal [Zn] and [B], as concentrations of these elements significantly differ between the two *Muricella* colonies (Figures 3f and 3g). For Zn, significantly higher concentrations in the deepest *Muricella* colony could reflect ambient seawater concentrations as [Zn] is higher at middepths than in near-surface waters [*Bruland*, 1980]. This is unlikely, however, since the two *Muricella* colonies are only separated by 20 m in depth. For boron, significantly lower concentrations in the *Muricella* colony from 85 m are not consistent with known changes in [B] in seawater with depth. Therefore, higher [Zn] in the *Muricella* colony from 105 m and lower [B] in the *Muricella* colony from 85 m likely reflect colony-specific variability. Consequently, ambient concentrations of Zn and B likely do not drive skeletal concentrations across a depth transect, and thus these elements may have limited use for paleoceanographic reconstructions. Additional specimens from these taxa are needed to further quantify colony-specific and order-specific variability.

4.2. Laser Ablation ICP-MS Radial Profiles of Element Intensities

[29] Laser ablation ICP-MS radial transects were highly reproducible for all elements measured in the *Antipathes* colony from 5 m (Figure 5). This suggests a common influence on the elemental composition of skeleton formed at the same time, regardless if this is biologically or environmentally driven.

[30] Lower laser ablation-derived $^{79}Br/^{13}C$ intensities and higher $^{127}I/^{13}C$ intensities in the oldest part of the *Antipathes* skeleton (Figures 5a and 5b) are consistent with higher [I] and lower [Br] in the older parts of an *Antipathes* skeleton reported by *Goldberg* [1978] using neutron activation analysis. In black corals, higher concentrations of I are associated with gluing regions between cells in the skeleton [*Nowak et al.*, 2009]. Thus, the high I concentrations in the oldest parts of the skeleton (Figure 5b) [*Goldberg*, 1978] indicate elevated percentage of gluing regions related to the early stages of growth. The similarities in the intensity profiles of $^{208}Pb/^{13}C$, $^{55}Mn/^{13}C$, and $^{114}Cd/^{13}C$ with $^{127}I/^{13}C$ indicate that these elements may also be concentrated in the gluing zones in the early part of the record as well (Figures 5a and 5c–5e). Therefore, the distribution of many elements in the skeleton may reflect skeletal morphology and not be related to changes in ambient concentrations or environmental conditions at all. This interpretation contrasts with the interpretation of the solution ICP-MS measurements where [Mn] and [Cd] vary between the colonies in a manner consistent with ambient concentrations of the elements. Together, these data suggests that ambient environmental concentrations may determine the average concentrations of these elements in a colony while biology may drive compositional variability within that colony over time.

[31] *Nowak et al.* [2009] also reported high [Zn] in the gluing zones. This is not supported here where $^{64}Zn/^{13}C$ intensities were not elevated in the oldest portion of the record (Figure 5e). Thus, either skeletal [Zn] varies with black coral taxa or concentrations in the skeleton are environmentally driven. Combined with the solution ICP-MS measurements suggesting that [Zn] were colony specific, [Zn] in the skeleton are either colony-specific or taxa-specific effects.

[32] $^{11}B/^{13}C$ intensities fluctuated dramatically on interannual to decadal time scales throughout the *Antipathes* record (Figure 5g). Therefore, although ambient B concentrations may not determine average concentrations of a given colony across a depth transect, variations in [B] at a single depth may drive compositional variability within that colony over time. Thus, [B] may be the most promising possibility for trace element reconstructions of all of the elements in this study. Despite the large-scale relationship between [B] concentration and salinity [*Barth*, 1998; *Lee et al.*, 2010], the $^{11}B/^{13}C$ record did not correlate with seawater salinity reconstructed from a nearby coral [*Iijima et al.*, 2005]. Therefore, a better understanding of the drivers of the B concentration associated with POM, seawater, and the coral skeleton are needed before the [B] record here can be interpreted with confidence.

[33] In contrast to the *Antipathes* colony, no reproducible or interpretable patterns in intensities of either $^{79}Br/^{13}C$ or $^{127}I/^{13}C$ were measured by laser ablation in the *Muricella* colonies (Figures 6a, 6b, 7a, and 7b). This, in addition to the low degree of reproducibility of the radial transects in the *Muricella* colonies for nearly all of the elements measured (Figures 6 and 7) suggests that it is not possible to extract reliable paleoceanographic records from the skeleton of *Muricella* corals by LA ICP-MS at this time.

4.3. Implications for LA ICP-MS Paleoceanographic Reconstructions

[34] Symmetrical growth and high reproducibility among radial transects in the *Antipathes* colony indicate that these corals may be useful for high-resolution trace element paleoceanographic reconstructions by LA ICP-MS. The next logical steps toward using trace elements in *Antipathes* for paleoceanographic reconstructions include (1) validating ^{13}C as an internal standard, (2) testing the hypothesis that trace elements are incorporated into azooxanethallate corals taxa via POM rather than assimilated from dissolved elements in seawater, and (3) calibrating the skeletal trace elements with ambient environmental concentrations. In contrast to *Antipathes*, asymmetrical growth bands and high skeletal heterogeneity in the *Muricella* colonies are a limiting factor in developing LA ICP-MS proxies from the skeleton of this genus. Overall, this work provides initial data in support of further development of proxy records using high-resolution trace element measurements by ICP-MS in *Antipathes* corals.

Acknowledgments

[35] We thank P. Colin and L. Colin at the Coral Reef Research Foundation for collecting the two *Muricella* colonies and assistance with collecting the *Antipathes* colony. J. Olesik and A. Lutton from the Trace Element Research Lab, C. Begg from the Campus Electron Optics Facility, and C. Millan provided laboratory support. S. Levas, R. Moyer, and B. Thibodeau offered insightful comments on this research. We also thank two anonymous reviewers for their comments. B. Williams was supported by an NSERC postgraduate scholarship and received additional funding from PADI Foundation, the Geological Society of America, Friends of Orton Hall, and American Women in Science. Laboratory analyses were funded by National Science Foundation Chemical Oceanography (0610487 and 0426022) and National Science Foundation Biological Oceanography (0542415) to A. G. Grottoli.

References

Abe, K. (2004), Cadmium distribution in the western Pacific, in *Global Environmental Change in the Ocean and on Land*, edited by M. Shiyomi et al., pp. 189–203, Terrapub, Tokyo.

Barth, S. (1998), $^{11}B/^{10}B$ variations of dissolved boron in a freshwater-seawater mixing plume (Elbe Estuary, North Sea), *Mar. Chem.*, *62*(1–2), 1–14, doi:10.1016/S0304-4203(98)00023-1.

Beck, J., R. Edwards, E. Ito, F. Taylor, J. Recy, F. Rougerie, P. Joannot, and C. Henin (1992), Sea-surface temperature from coral skeletal strontium/calcium ratios, *Science*, *257*, 644–647, doi:10.1126/science.257.5070.644.

Bond, Z., A. Cohen, S. Smith, and W. Jenkins (2005), Growth and composition of high-Mg calcite in the skeleton of a Bermudian gorgonian (*Plexaurella dichotoma*): Potential for paleothermometry, *Geochem. Geophys. Geosyst.*, *6*, Q08010, doi:10.1029/2005GC000911.

Boyle, E., F. Sclater, and J. Edmond (1976), On the marine geochemistry of cadmium, *Nature*, *263*, 42–44, doi:10.1038/263042a0.

Bruland, K. (1980), Oceanographic distributions of cadmium, zinc, nickel and copper in the North Pacific, *Earth Planet. Sci. Lett.*, *47*, 176–198, doi:10.1016/0012-821X(80)90035-7.

Bruland, K. (1983), Trace elements in sea-water, in *Chemical Oceanography*, edited by J. P. Riley and R. Chester, pp. 157–220, Academic, London.

Colin, P. (2001), Water temperature on the Palauan reef tract: Year 2000, *CRRF Tech. Rep., 1*, 17 pp., Coral Reef Res. Found., Koror, Palau.

Cook, F. (1904), The chemical composition of some gorgonian corals, *Am. J. Physiol.*, *12*, 95–98.

Couch, E. (1971), Calculation of paleosalinities from boron and clay mineral data, *Am. Assoc. Pet. Geol. Bull.*, *55*, 1829–1837.

Delcroix, T., C. Henin, V. Porte, and P. Arkin (1996), Precipitation and sea-surface salinity in the tropical Pacific Ocean, *Deep Sea Res., Part 1*, *43*(7), 1123–1141.

Fabricius, K., and P. Alderslade (2001), *Soft Corals and Sea Fans: A Comprehensive Guide to the Tropical Shallow Water Genera of the Central-West Pacific, the Indian Ocean and the Red Sea*, 264 pp., Aust. Inst. of Mar. Sci., Townsville, Queensl., Australia.

Fisher, N., J.-L. Teyssie, S. Krishnaswami, and M. Baskaran (1987), Accumulation of Th, Pb, U, and Ra in marine phytoplankton and its geochemical significance, *Limnol. Oceanogr.*, *32*(1), 131–142, doi:10.4319/lo.1987.32.1.0131.

Flegal, A., and C. Patterson (1983), Vertical concentration profiles of lead in the central Pacific at 15°N and 20°S, *Earth Planet. Sci. Lett.*, *64*(1), 19–32, doi:10.1016/0012-821X(83)90049-3.

Goldberg, W. (1976), Comparative study of the chemistry and structure of Gorgonian and Antipatharian coral skeletons, *Mar. Biol. Berlin*, *35*, 253–267, doi:10.1007/BF00396873.

Goldberg, W. (1978), Chemical changes accompanying maturation of the connective tissue skeletons of Gorgonian and Antipatharian corals, *Mar. Biol. Berlin*, *49*, 203–210, doi:10.1007/BF00391132.

Goldberg, W., T. Hopkins, S. Holl, J. Schaefer, K. Kramer, T. Morgan, and K. Kim (1994), Chemical composition of the sclerotized black coral skeleton (Coelenterata: Antipatharia): A comparison of two species, *Comp. Biochem. Physiol.*, *107*(4), 633–643, doi:10.1016/0305-0491(94)90197-X.

Grange, K., and W. Goldberg (1994), Chronology of black coral growth bands: 300 years of environmental history?, paper presented at the Second International Temperate Reef Symposium, Natl. Inst. of Water and Atmos. Res., Auckland, New Zealand.

Härdstedt-Roméo, M. (1982), Some aspects of the chemical composition of plankton from the north-western Mediterranean Sea, *Mar. Biol. Berlin*, *70*, 229–236, doi:10.1007/BF00396841.

Heron, S., E. Metzger, and W. Skirving (2006), Seasonal variations of the ocean surface circulation in the vicinity of Palau, *J. Oceanogr.*, *62*, 413–426, doi:10.1007/s10872-006-0065-3.

Iijima, H., H. Kayanne, M. Morimoto, and O. Abe (2005), Interannual sea surface salinity changes in the western Pacific

from 1954 to 2000 based on coral isotope analysis, *Geophys. Res. Lett.*, *32*, L04608, doi:10.1029/2004GL022026.

Klinkhammer, G., and M. Bender (1980), The distribution of manganese in the Pacific Ocean, *Earth Planet. Sci. Lett.*, *46*(3), 361–384, doi:10.1016/0012-821X(80)90051-5.

Lea, D., G. Shen, and E. Boyle (1989), Coralline barium records temporal variability in equatorial Pacific upwelling, *Nature*, *340*, 373–376, doi:10.1038/340373a0.

Lee, K., T.-W. Kim, R. H. Byrne, F. J. Millero, R. A. Feely, and Y.-M. Liu (2010), The universal ratio of boron to chlorinity for the North Pacific and North Atlantic oceans, *Geochim. Cosmochim. Acta*, *74*(6), 1801–1811, doi:10.1016/j.gca.2009.12.027.

Lewis, S., G. Shields, B. Kamber, and J. Lough (2007), A multi-trace element coral record of land-use changes in the Burdekin River catchment, NE Australia, *Palaeogeogr. Palaeoclimatol. Palaeoecol.*, *246*, 471–487, doi:10.1016/j.palaeo.2006.10.021.

Matthews, K., A. Grottoli, W. McDonough, and J. Palardy (2008), Upwelling, species, and depth effects on coral skeletal cadmium-to-calcium ratios (Cd/Ca), *Geochim. Cosmochim. Acta*, *72*(18), 4537–4550, doi:10.1016/j.gca.2008.05.064.

Moore, R., F. Bayer, H. Boschma, H. Harrington, D. Hill, L. Hyman, M. Lecompte, E. Gallitelli, E. Stumm, and J. Wells (Eds.) (1956), *Treatise on Invertebrate Paleontology*, part F, *Coelenterata*, 498 pp., Geol. Soc. of Am., New York.

Morris, A., and J. Riley (1966), The bromide/chlorinity and sulphate/chlorinity ratio in sea water, *Deep Sea Res.*, *13*, 699–705.

Nowak, D., M. Florek, J. Nowak, W. Kwiatek, J. Lekki, E. Zieba, P. Romero, B. Ben-Nissan, and A. Kuczumow (2005), Micro-spectrometric investigations of inorganic components of the black corals for biomedical applications, *Key Eng. Mater.*, *284–286*, 297–300, doi:10.4028/www.scientific.net/KEM.284-286.297.

Nowak, D., et al. (2009), Morphology and the chemical make-up of the inorganic components of black corals, *Mater. Sci. Eng. C*, *29*(3), 1029–1038, doi:10.1016/j.msec.2008.08.028.

Picaut, J., M. Ioualalen, C. Menkes, T. Delcroix, and M. McPhaden (1996), Mechanism of the zonal displacements of the Pacific Warm Pool: Implications for ENSO, *Science*, *274*(5292), 1486–1489, doi:10.1126/science.274.5292.1486.

Rege, S., S. Jackson, W. Griffin, R. Davies, N. Pearson, and Y. O'Reilly (2005), Quantitative trace-element analysis of diamond by laser ablation inductively coupled plasma mass spectrometry, *J. Anal. At. Spectrom.*, *20*, 601–611, doi:10.1039/b501374g.

Roche, J. (1952), Biochemie comparee des scleroproteines iodees des anthozoaries et des spongiares, *Experientia*, *8*, 45–54, doi:10.1007/BF02139015.

Shen, G., E. Boyle, and D. Lea (1987), Cadmium in corals as a tracer of historical upwelling and industrial fallout, *Nature*, *328*, 794–796, doi:10.1038/328794a0.

Sherwood, O., and M. Risk (2007), Deep-sea corals: New insights to paleoceanography, in *Proxies in Late Cenozoic Paleoceanography*, *Dev. in Mar. Geol.*, vol. 1, edited by C. Hillaire-Marcel and A. De Vernal, pp. 491–522, Elsevier, Amsterdam.

Sherwood, O., D. Scott, M. Risk, and T. Guilderson (2005a), Radiocarbon evidence for annual growth rings in a deep sea octocoral (*Primnoa resedaeformis*), *Mar. Ecol. Prog. Ser.*, *301*, 129–134, doi:10.3354/meps301129.

Sherwood, O., J. Heikoop, D. Sinclair, D. Scott, M. Risk, and C. Shearer (2005b), Skeletal Mg/Ca in *Primnoa resedaeformis*: Relationship to temperature?, in *Cold Water Corals and Ecosystems*, edited by A. Freiwald and M. Roberts, pp. 1061–1079, doi:10.1007/3-540-27673-4_53, Springer, Berlin.

Smith, S., R. Buddemeier, R. Redalje, and J. Houck (1979), Strontium-calcium thermometry in coral skeletons, *Science*, *204*(4391), 404–407, doi:10.1126/science.204.4391.404.

Sugimoto, K. (1928), Iodine in gorgonian corals, *J. Biol. Chem.*, *76*(3), 723–728.

Tudhope, A., D. Lea, G. Shimmield, C. Chilcott, T. Scoffin, A. Fallick, and M. Jebb (1997), Climate records from massive Porites corals in Papua New Guinea: A comparison of skeletal Ba/Ca, skeletal $\delta^{18}O$ and coastal rainfall, paper presented at the 8th International Coral Reef Symposium, Univ. of Panama, Panama City.

Weinbauer, M., and B. Velimirovm (1995), Calcium, magnesium and strontium concentrations in the calcite sclerites of Mediterranean gorgonians (Coelenterata: Octocorallia), *Estuarine Coastal Shelf Sci.*, *40*, 87–104, doi:10.1016/0272-7714(95)90015-2.

Williams, B., and A. Grottoli (2010a), Recent shoaling of the nutricline and thermocline in the western tropical Pacific, *Geophys. Res. Lett.*, *37*, L22601, doi:10.1029/2010GL044867.

Williams, B., and A. Grottoli (2010b), Stable nitrogen and carbon isotopic ($\delta^{15}N$ and $\delta^{13}C$) variability in shallow tropical Pacific soft coral and black coral taxa and implications for paleoceanographic reconstructions, *Geochim. Cosmochim. Acta*, *74*(18), 5280–5288, doi:10.1016/j.gca.2010.5206.5026.

Williams, B., M. Risk, S. Ross, and K. Sulak (2007), Stable isotope records from deep-water Antipatharians: 400-year records from the south-eastern coast of the United States of America, *Bull. Mar. Sci.*, *81*(3), 437–447.

Xu, Y., L. Feng, P. Jeffrey, Y. Shi, and F. Morel (2008), Structure and metal exchange in the cadmium carbonic anhydrase of marine diatoms, *Nature*, *452*, 56–61, doi:10.1038/nature06636.

Yoshikawa, C., Y. Yamanaka, and T. Nakatsuka (2006), Nitrate-nitrogen isotopic patterns in surface waters of the western and central equatorial Pacific, *J. Oceanogr.*, *62*, 511–525, doi:10.1007/s10872-006-0072-4.

Zhang, R., A. Busalacchi, and Y. Xue (2007), Decadal change in the relationship between the oceanic entrainment temperature and thermocline depth in the far western tropical Pacific, *Geophys. Res. Lett.*, *34*, L23612, doi:10.1029/2007GL032119.